RESEARCH ARTICLE

Key Points:
- Salt water incursion alters Fe and S cycling in wetland soils
- Soil Fe pools buffer against salt water incursion
- Fe-S interactions determine sulfidic soil thresholds

Correspondence to:
A. J. Burgin,
aburgin2@unl.edu

Iron clad wetlands: Soil iron-sulfur buffering determines coastal wetland response to salt water incursion

Valerie A. Schoepfer[1], Emily S. Bernhardt[2], and Amy J. Burgin[1]

[1]School of Natural Resources, University of Nebraska-Lincoln, Lincoln, Nebraska, USA, [2]School of Biological Sciences, Duke University, Durham, North Carolina, USA

Abstract Coastal freshwater wetland chemistry is rapidly changing due to increased frequency of salt water incursion, a consequence of global change. Seasonal salt water incursion introduces sulfate, which microbially reduces to sulfide. Sulfide binds with reduced iron, producing iron sulfide (FeS), recognizable in wetland soils by its characteristic black color. The objective of this study is to document iron and sulfate reduction rates, as well as product formation (acid volatile sulfide (AVS) and chromium reducible sulfide (CRS)) in a coastal freshwater wetland undergoing seasonal salt water incursion. Understanding iron and sulfur cycling, as well as their reduction products, allows us to calculate the degree of sulfidization (DOS), from which we can estimate how long soil iron will buffer against chemical effects of sea level rise. We show that soil chloride, a direct indicator of the degree of incursion, best predicted iron and sulfate reduction rates. Correlations between soil chloride and iron or sulfur reduction rates were strongest in the surface layer (0–3 cm), indicative of surface water incursion, rather than groundwater intrusion at our site. The interaction between soil moisture and extractable chloride was significantly related to increased AVS, whereas increased soil chloride was a stronger predictor of CRS. The current DOS in this coastal plains wetland is very low, resulting from high soil iron content and relatively small degree of salt water incursion. However, with time and continuous salt water exposure, iron will bind with incoming sulfur, creating FeS complexes, and DOS will increase.

1. Introduction

In the coming decades, large areas of coastal wetlands will change from freshwater-dominated systems to salt water-dominated systems through the drivers of climate change and resulting sea level rise [*Poulter and Halpin*, 2008]. Inland drought and changing precipitation patterns, frequently associated with climate change, drive seawater incursion [*Ardón et al.*, 2013; *Werner et al.*, 2013]. With frequent and intensified incursion, a coastal freshwater wetland has the potential to transition to a salt water wetland, given the appropriate sea levels and chemical conditions over a necessary time frame [*Craft et al.*, 2009; *Megonigal and Neubauer*, 2009]. The transition from a freshwater-dominated system to a salt water-dominated system often signifies a loss in plant and microbial diversity as well as ecosystem services, such as nitrogen sequestration, denitrification, and aboveground biomass [*Brock et al.*, 2005; *Craft et al.*, 2009; *Odum*, 1988].

Sea water incursion increases salinity but also alters sulfate concentrations by orders of magnitude as full-strength seawater has 10–1000X more sulfate than freshwaters [*Lamers et al.*, 2013]. Sulfate reduction to sulfide, via microbial respiration, follows nitrate and iron reduction as the next most thermodynamically favorable reaction to microbes [*Stumm and Morgan*, 1996]. As excess sulfide is produced, it has the potential to chemically transform an ecosystem to a more sulfide tolerant plant and microbial community [*Pezeshki*, 2001; *Wang and Chapman*, 1999].

Under the pressure of sea level rise, the transition from coastal freshwater to saline wetlands is inevitable, but natural chemical mechanisms can alter the time course and severity of this transition. Iron plays a major role in buffering freshwater wetlands against the shift toward a sulfide tolerant plant and microbial community [*van der Welle et al.*, 2006, 2007]. In the coastal southeastern United States, iron is the dominant element in Ultisol soils, and iron reduction is potentially the dominant anaerobic respiratory pathway [*Lovley*, 1991; *Neubauer et al.*, 2005; *Weston et al.*, 2006]. Iron hydroxide (an oxidized compound containing iron (III)) is insoluble in pure water [*Lovley*, 1991]. However, with an increase in salinity and coastal derived organic
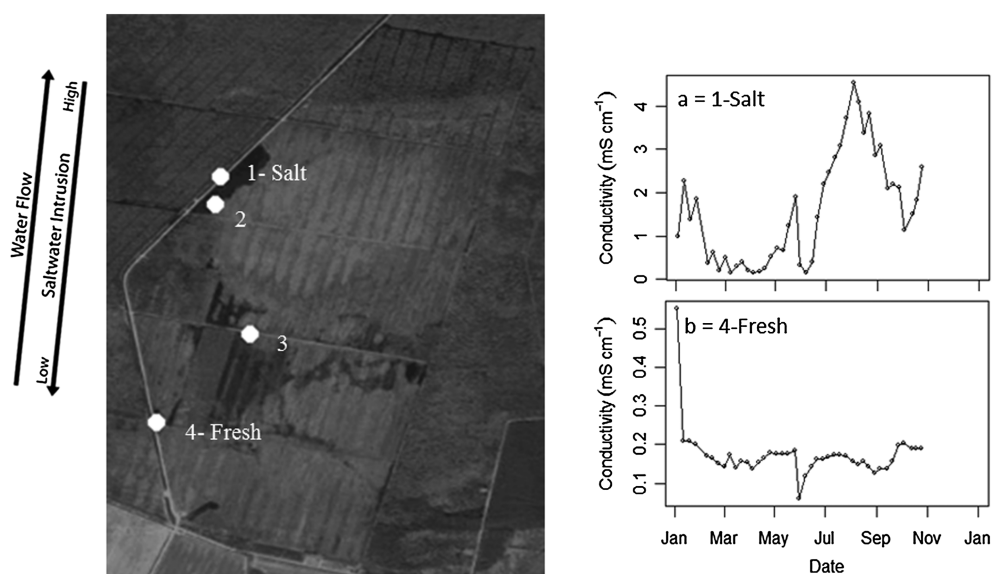
Figure 1. Map of Timberlake Observatory for Wetland Restoration (TOWeR), North Carolina, USA. The white dots represent the sampling locations. Weekly surface water conductivity over 2012 at (a) Site 1 (salt) and (b) Site 4 (fresh) demonstrates the spatial extremes of the incursion event. Note the 10X difference in *y* axes.

ligands, iron (III) becomes aqueous [*Liu and Millero*, 1999, 2002; *Weston et al.*, 2006]. In order for microbial reduction to iron (II) to occur, iron must be in this aqueous state [*Lovley*, 1991]. Wetlands are high in organic ligands, and the combination of these ligands and sodium chloride from salt water incursion greatly enhances the potential for iron reduction, the product of which is reduced iron (II). Iron (II) can occur at very high concentrations in reduced freshwater wetland sediments [*Donahoe and Liu*, 1998].

Reduced iron (II) and sulfide chemically bind to create iron sulfide (FeS) compounds, which are relatively unavailable to biota [*Connell and Patrick*, 1968; *Morse et al.*, 2007] and are responsible for buffering soils from sulfide accumulation [*Wijsman and Middelburg*, 2001]. FeS complexes are nontoxic and are easily oxidized in the early stages of formation [*King and Nedwell*, 1985; *Lord and Church*, 1983; *van der Welle et al.*, 2007]. With time and increased sulfide, these complexes become metastable and eventually are replaced by compounds such as pyrite (FeS_2), which can withstand exposure to oxygen [*Rabenhorst et al.*, 2010]. Sulfide sequestration is defined by the amount of sulfide in the sediment system relative to iron and is termed the degree of sulfidization [*Burton et al.*, 2006; *Huerta-Diaz et al.*, 1998; *Morse et al.*, 2007]. A simple model incorporating DOS and current sea levels could allow for a conservative timeline determining when coastal wetlands will begin the transition from a freshwater dominated community to a net sulfidic system.

In this study, we asked the following: In a southeastern (U.S.) wetland experiencing salt water incursion, how does the sedimentary iron pool buffer against the chemical effects of seasonal salt water incursion? We hypothesized that the biogeochemical interactions between sulfur and iron cycling would in part determine the transition of the soils to a net sulfidic system. We measured iron and sulfur reduction rates and their end-products over a period of salt water incursion. Several predictor variables indicative of soil and surface water chemistry were assessed to determine controls on iron and sulfur cycling, as well as on the degree of sulfidization (DOS). We hypothesized that pore water chloride, indicative of the amount of salt water on the site, would be the best predictor of sulfidization (DOS). Our study provides increased understanding of how sedimentary iron can buffer against salt water incursion at the Timberlake wetland.

2. Materials and Methods

2.1. Field Site Description and Sample Collection

The Timberlake Observatory for Wetland Restoration (TOWeR) is a large (440 ha) wetland located in the Albermarle-Pamlico Peninsula in coastal North Carolina in Tyrrell County (Figure 1). This wetland is protected from high salinity by constant freshwater discharge and barrier islands along the coastline. Hydrologic
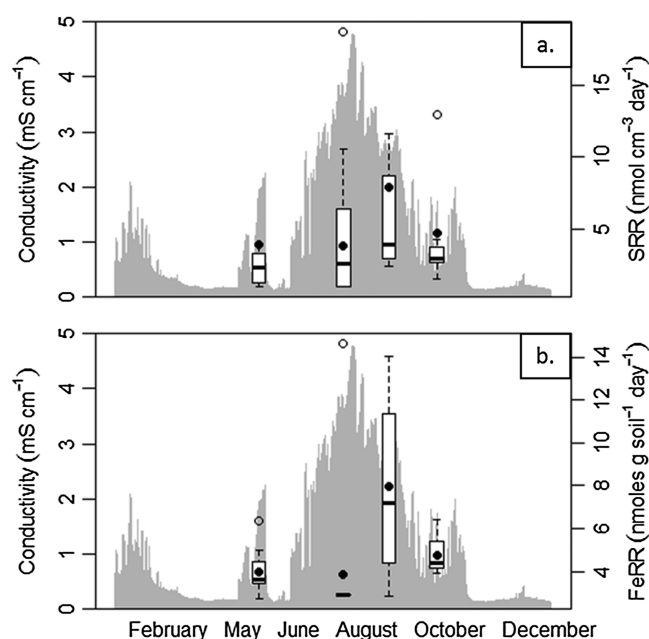
Figure 2. Grey background denotes specific conductivity at the salt site (Site 1, nearest salt water source) in 2012. Overlain are boxplots of back-transformed (a) sulfate reduction rates (SRR) (n = 99, 99, 87, and 70 in May July, August, and October) and (b) iron reduction rates (FeRR) (n = 197, 196, 186, and 196 in May, July, August, and October) over all sites and 0–3 cm during each sampling period. The middle line represents the median, and the black point represents the mean of the back-transformed data.

variation, including decreased precipitation, increased evaporation, and agricultural pumping for irrigation, cause summer surface water-driven episodes of salt water intrusion [*Ardón et al.*, 2013, Figure 1]. Maximum salinity reaches around 5 parts per thousand at the height of incursion at the "salt" site, which creates a salinity gradient toward freshwater portions of the site ("fresh"; Figures 1 and 2). Site characteristics and history are discussed in more detail by *Ardón et al.* [2010] and *Morse et al.* [2012].

In May, July, August, and October 2012, we collected duplicate 30 cm long, 5 cm diameter soil cores at four locations throughout the TOWeR wetland (Figure 1, white dots) and immediately transported them on ice to the University of Nebraska-Lincoln within 24 h of collection. Sampling sites represent the longitudinal (salt to fresh) gradient at the larger site (Figure 1). Vegetation along the channel ranges from (Site 1) sparsely forested, (Sites 2 and 3) densely herbaceous, and slightly shrubby to (Site 4) slightly shrubby [*Hopfensperger et al.*, 2014]. Cores were sectioned under anaerobic conditions (Coy Anaerobic Chamber, Coy Products) and homogenized into the 0–3, 3–6, and 6–9 cm depths. Subsamples from each depth were analyzed for iron reduction potential, sulfate reduction rates, FeS complex concentration (as acid volatile sulfide (AVS) and chromium reducible sulfide (CRS)), and total iron content. We also quantified soil moisture, bulk density, and water extractable chloride and sulfate concentrations for each depth section.

2.2. Soil Iron and Sulfur Analyses

We determined iron (Fe) reduction potential by a modification of *Neubauer et al.*'s [2005] methods, which involved anaerobically adding 2 g of soil from each depth and site to a 20 mL scintillation vial filled with 15 mL of deoxygenated site water. Sodium molybdate (20 mmol final concentration) was added to inhibit sulfate reduction in a subset of the vials. Shaking the vials for 5 days underwater at room temperature ensured a homogenized sample with maximum ambient microbial activity. Anaerobically removing a 0.5 mL slurry subsample each day from the vial into 5 mL of a 0.5 molar hydrochloric acid solution transformed iron (II) (s) to iron (II) (aq). From this solution, we added a 1 mL subsample to a solution of ferrozine and HEPES [*Lovley and Phillips*, 1986] and read samples and blanks colorimetrically at 552 nm (detection limit = 4.5 nmol L^{-1}). We determined reduction rates from a linear regression of the change in iron (II) concentration over time in units of mg Fe (II) dry g^{-1} h^{-1} [*Neubauer et al.*, 2005].

We measured sulfate (SO_4^{2-}) reduction rates with $^{35}SO_4^{2-}$ [*Fossing and Jørgensen*, 1989]. We added 5 g of sediment from each depth and site to triplicate 60 mL vials and injected them with 1 mL of a 1 μ Cu/mL $^{35}SO_4^{2-}$ solution. Flushing the vials with helium removed the excess hydrogen (a preferential electron donor, present in the anaerobic chamber gas mixture). After room temperature anaerobic incubation for 12–16 h, the resulting sulfide was fixed by injecting 5 mL 20% zinc acetate and immediately freezing. We used the cold chromium reducible sulfur technique (CRS, mean recovery = 88.6%) [*Fossing and Jørgensen*, 1989] to volatilize and trap the radiolabeled sulfide, half of which was subsequently analyzed on a liquid scintillation counter. We also measured the remaining sulfide concentration colorimetrically (detection limit = 37.5 nmol l^{-1}) [*Golterman*, 1991].

Table 1. All Geometric Mean Values for the 0–3 cm Depth at the Channel Sites Throughout the Incursion Season[a]

Site/Month Mean ± SE	FeRR nmol Fe g^{-1} d^{-1}	SRR nmol S cm^{-3} d^{-1}	AVS nmol S g^{-1}	CRS nmol S g^{-1}	Total Fe mmol Fe g^{-1}	Moisture Fraction	Extract. Cl$^-$ mmol Cl L^{-1}	Extract. SO$_4^{2-}$ mmol SO$_4^{2-}$ L^{-1}
			1 Salt					
May	19.17 ± 6.31	8.91 ± 5.12	19.31 ± 9.08	57.51 ± 30.33	150.01	0.80	4.04	2.59
July	0.38 ± 0.21	-	0.00 ± 0.00	67.00 ± 35.50	62.30	0.82	43.72	6.23
August	431.23 ± 21.55	243.41 ± 19.78	5.39 ± 5.39	250.25 ± 62.57	86.70	0.77	49.52	1.71
October	30.14 ± 15.71	15.61 ± 6.30	0.00 ± 0.00	49.25 ± 45.51	98.71	0.74	16.74	1.75
			2 Salt					
May	4.03 ± 2.02	8.78 ± 3.46	0.00 ± 0.00	106.27 ± 40.37	100.01	0.72	7.34	2.13
July	0.05 ± 0.07	183.04 ± 45.79	0.00 ± 0.00	60.00 ± 50.00	52.80	0.69	5.03	1.10
August	175.26 ± 117.53	52.69 ± 20.52	0.00 ± 0.00	136.07 ± 71.71	102.50	0.72	32.46	1.22
October	25.23 ± 5.15	123.90 ± 119.16	0.00 ± 0.00	77.98 ± 39.29	-	0.60	12.32	0.91
			3 Salt					
May	31.28 ± 15.35	-	0.00 ± 0.00	-	191.84	0.62	2.70	0.33
July	0.03 ± 0.11	18.37 ± 6.78	0.00 ± 0.00	1.63 ± 1.63	0.77	0.61	2.32	0.42
August	63.08 ± 37.37	14.50 ± 4.01	0.00 ± 0.00	0.00 ± 0.00	70.23	0.65	3.85	0.33
October	33.68 ± 8.10	10.62 ± 0.37	0.00 ± 0.00	0.00 ± 0.00	69.85	0.59	2.01	0.18
			4 Fresh					
May	9.33 ± 5.97	16.39 ± 2.58	0.00 ± 0.00	4.47 ± 0.87	948.04	0.56	1.20	0.41
July	0.24 ± 0.04	427.01 ± 416.44	0.00 ± 0.00	4.97 ± 2.49	28.46	0.46	0.79	0.28
August	77.29 ± 40.57	10.02 ± 1.90	0.00 ± 0.00	0.00 ± 0.00	210.44	0.45	0.51	0.15
October	14.12 ± 2.30	18.63 ± 1.88	0.00 ± 0.00	2.22 ± 2.22	78.97	0.41	1.11	0.09

[a]All values are geometric mean ± standard error. FeRR = iron reduction rate, SRR = sulfate reduction rate, AVS = acid volatile sulfide, CRS = chromium reducible sulfur, and Extract. Cl = water extractable chloride. All mass units are in grams dry weight. A dash denotes missing samples.

In addition to CRS, we measured acid volatile sulfide (AVS, detection limit = 37.5 nmol L^{-1}) on two replicate soil samples from each section of the cores following a modified purge and trap procedure [*Allen et al.*, 1993]. Modification included a smaller manifold configuration rather than the large, singular trap. Total sediment iron samples were digested according to Environmental Protection Agency (EPA) protocol 3015a and were measured on a flame atomic absorption analyzer using EPA protocol 3111 (detection limit = 0.05 mg L^{-1}). This method included digesting a known amount of sediment in a microwave with hydrochloric and nitric acid, then diluting the sample and colorimetrically reading the flame produced when combusting with acetylene gas. Water extractable chloride and sulfate concentrations were quantified by adding a known amount of water to a known sediment sample, shaking and filtering the sample, and analyzing the extractant via ion chromatography. We calculated soil moisture by oven-drying a soil sample at 100°C overnight.

2.3. Degree of Sulfidization (DOS) Calculations

The proportion of total sulfide that is occupying iron in FeS compounds is known as the degree of sulfidization (DOS) [*Boesen and Postma*, 1988]. Practically, it is the CRS concentration divided by two to represent the molar amount of iron present in FeS$_2$ plus the AVS concentration multiplied by one (FeS) divided by the total iron content of the sediment [*Boesen and Postma*, 1988; *Burton et al.*, 2006]. Here we make the simplifying assumption that H$_2$S and elemental sulfur are negligible; we know that pore water H$_2$S is relatively low on the site due to previous work [*Hopfensperger et al.*, 2014]. This fraction ranges from 0 to 1; a value above 1 indicates excess free sulfide (e.g., site is in a "sulfidic" state), while DOS < 1 implies that there is still available iron left for binding.

$$\text{DOS} = \frac{\text{Fe(sulfide)}}{\text{Fe(total)}} = \frac{\text{CRS}_{\text{Fe}} + \text{AVS}_{\text{Fe}}}{\text{Total Fe}}$$

2.4. Statistical Analysis

We were interested in determining the controls on the response variables of (1) iron reduction rates, (2) sulfate reduction rates, (3) acid volatile sulfide concentrations, and (4) chromium reducible sulfur concentrations and
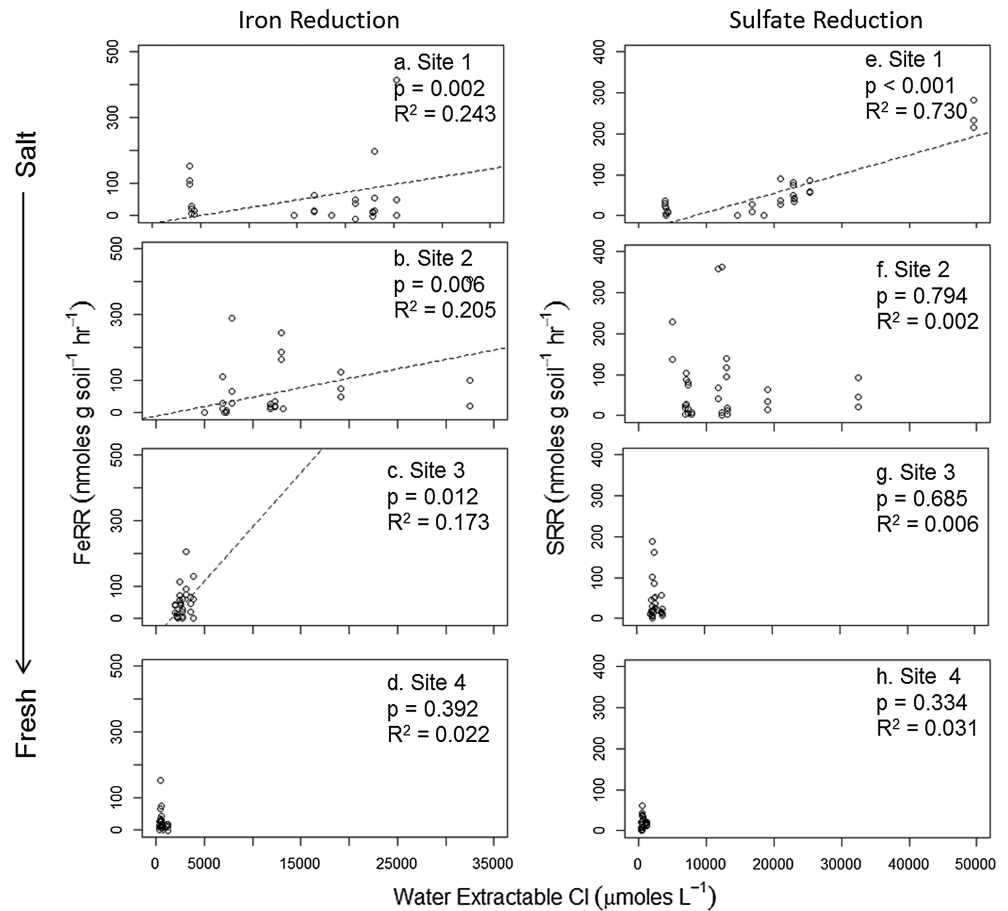
Figure 3. Untransformed (a–d) iron reduction rates (FeRR) and (e–h) sulfate reduction rates (SRR) as predicted by water extractable chloride in the permanently flooded sites ranging from closest to the salt water source (1) to furthest from the source (4).

determine the cause of any significant differences in the means of each response variable. All statistical analyses were performed in *R* using base packages [*R Core Team*, 2012]. Correlations were run between all pairs of potential control (predictor) variables, including month, depth, water extractable chloride, water extractable sulfate, water extractable dissolved organic carbon, pore water chloride, pore water sulfate, total iron content, days inundated, and soil moisture. Variables were removed for autocorrelation with $r > 0.35$. Many potential predictor variables were eliminated due to autocorrelation. For example, although the month was often a significant categorical factor in statistical analyses, it was eliminated due to its correlation with pore water chloride content ($r = -0.61$). Final predictor variables for model inputs included (1) water extractable chloride (indicative of the degree of salt water incursion) and (2) soil moisture (indicative of hydrologic variation). Analysis of variance (ANOVA) determined which predictor variables controlled a given response variable. All response variables were $\log + 1$ transformed before testing significance via ANOVA ($\alpha = 0.05$). After transformation, all ANOVA assumptions were met including normally distributed residuals and equal variance. Multiple linear regressions were used to model the relationships between the response and predictor variables and determine how predictive each variable was to the response. Outliers were determined to be any data point $>1.5X$ the interquartile range of the data set and were removed to minimize skewing regression relationships.

3. Results

The degree of summer salt water incursion was recorded by monitoring the conductivity at multiple locations in TOWeR in 2012. Conductivity ranged from ~0.6 to 4.7 m S/cm at Site 1 (salt) and 0.1 to 0.6 m S/cm at Site 4 (fresh) during the late summer to early fall dry period (Figure 1; weekly grab sample data set). Iron and sulfate reduction rates varied throughout the course of incursion (Figure 2; 15 min interval conductivity sample).
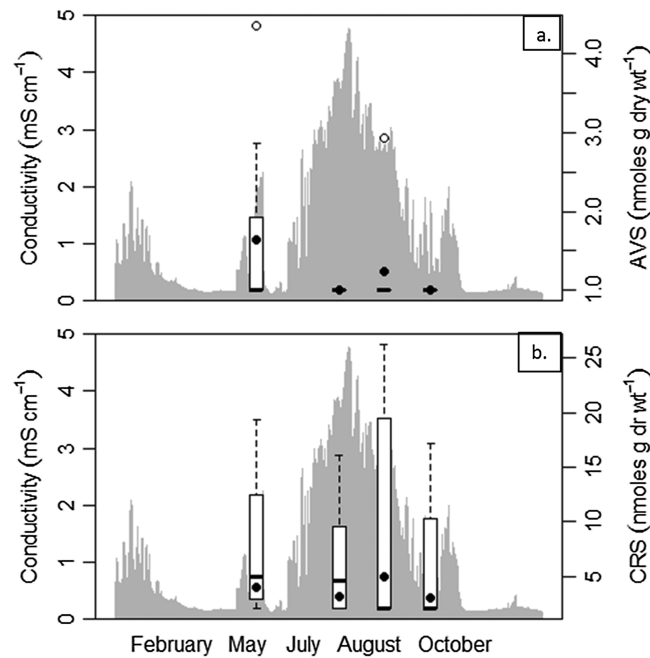
Figure 4. Specific conductivity at the downstream site over 2012. Overlain are boxplots of back-transformed (a) acid volatile sulfide ($n = 55, 66, 66$, and 66, in May, July, August, and October) and (b) chromium reducible sulfide ($n = 67, 95, 99$, and 99 in May, July, August, and October) over all sites during each sampling period. The middle line represents the median, and the black dot represents the mean of the back-transformed data.

Sulfate reduction rates followed a similar pattern to the rise and fall of conductivity, increasing in sites and at times of salt water exposure (Figure 2a; one-way ANOVA between sulfate reduction rates by month; d.f. = 3125; $f = 5.22$; $p = 0.002$). Rates were lowest and least variable in May with increased rates in July and August followed by decreased rates in October (Table 1). Iron reduction followed a similar pattern, with the exception of July's median rate, which was markedly lower (Table 1 and Figure 2b). Iron reduction rates were not significantly different between vials treated with sodium molybdate or not (one-way ANOVA, d.f. = 1772; $f = 0.003$; $p = 0.954$), and therefore, only data from unamended samples were used. Iron reduction rates ranged from a high in August, followed by rates measured in May, October, and July (Table 1).

Iron reduction rate (FeRR) and sulfate reduction rate (SRR) were individually regressed against chloride by site (compiled over all sampling dates, Figure 3). Water extractable chloride was strongly related to both sulfate and iron reduction rates at Site 1, which experienced the strongest incursion effects (Figures 3a and 3e). The relationship between water extractable chloride and sulfate reduction rates broke down for sites with less exposure to salt water (Figures 3f–3h). However, a significant relationship between water extractable chloride and iron reduction rates occurred at Sites 2 and 3 but was absent at Site 4 (freshest; Figures 3b–3d).

Median acid volatile sulfide and chromium reducible sulfur concentrations decreased over the summer months (Figure 4; 15 min interval conductivity sample). Acid volatile sulfide concentrations were only above detection in May. Chromium reducible sulfide had the highest variation across sites in August followed by highest geometric mean values in May, July, and October (Table 1 and Figure 4). The statistical interaction

Table 2. Significant Factors for Explaining Iron Reduction Rates (FeRR), Acid Volatile Sulfide (AVS), or Chromium Reducible Sulfide (CRS) Using a Multiple Regression Model With Soil Moisture and Water Extractable Chloride (Extract. Cl) as Predictor Variables[a]

Response/Predictor	Slope	Standard Error	d.f.	P Value	Multiple R^2
		FeRR			
Extract. Cl[*b] Moisture	−2.522e-4	1.031e-4	3143	0.016	0.102
SRR					
Extract. Cl	0.886	0.361	1127	0.015	0.045
		AVS			
Extract. Cl* Moisture	2.32e-4	9.01e-5	392	0.011	0.150
		CRS			
Extract. Cl	0.077	0.011	1134	<0.001	0.270
Moisture	0.153	0.032	1134	<0.001	0.148

[a]Prior to analysis, response variables were log + 1 transformed to correct nonnormality.
[b]Asterisks denote an interaction between two variables.
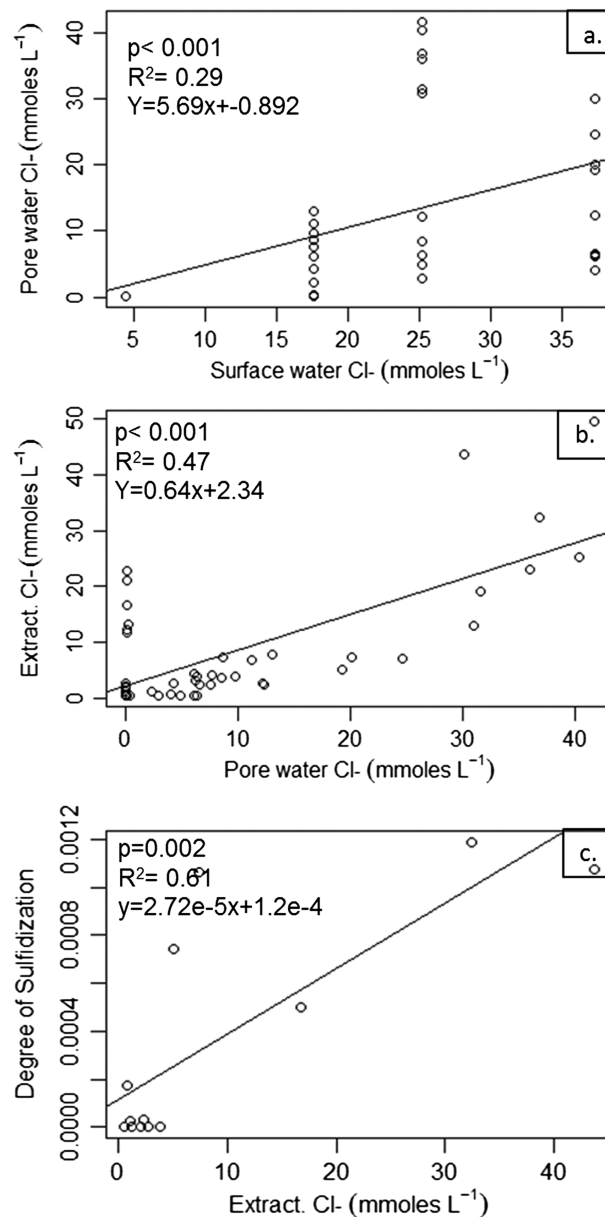
Figure 5. (a) Relationship between surface water chloride and soil pore water chloride across all sites and all sampling dates. (b) Relationship between pore water chloride and water extractable chloride and (c) degree of sulfidization (DOS) as a function of water extractable chloride across all sites at peak soil chloride (August). DOS is a unitless expression of the proportion soil iron occupied by sulfide. Any DOS values outside the whiskers of the DOS boxplot were eliminated from the figure.

between increasing soil moisture and water extractable chloride resulted in a significant increase in AVS concentration in the 0–3 cm depth across all sites as determined by multiple regression (Table 2). CRS significantly increased with increasing water extractable chloride and with increasing moisture.

Multiple regression models determined which variables (water extractable chloride or soil moisture) could significantly predict variation in iron or sulfate reduction rates (Table 2). In the multiple regression model, soil moisture and water extractable chloride explained significant variation in iron reduction rates (Table 2). Water extractable chloride significantly determined sulfate reduction rates.

Given the current chloride content and water budget for any wetland site, together with the relationship between chloride and DOS, it is possible to determine the chloride exposure needed to reach the DOS = 1 threshold, which represents the "tipping point" of the wetland into a sulfidic state. On our site, there is a significant relationship between surface water chloride and pore water chloride (Figure 5a), similarly, between pore water chloride and water extractable chloride (Figure 5b). By using these equations, we can determine that the approximate amount of water extractable chloride is associated with the concentration of chloride that enters the wetland over 1 year. Furthermore, there is a similarly strong relationship between water extractable chloride and the DOS value (Figure 5c), and this equation can predict the DOS under the given surface water chloride content. DOS and chloride content vary on an annual basis, as well as between years; thus, it is preferable to conceptualize this as a "lifetime" exposure necessary to tip the wetland into a sulfidic state. This lifetime load is the concentration of chloride that enters the site, summed over the course of the year, multiplied by the water that remains on the site (e.g., the inflow water—losses due to evaporation). If the difference between the current DOS and when DOS = 1 is small (1 and 2 orders of magnitude), a proportion can be solved for how much water extractable chloride is necessary for DOS = 1. In the case of our site, there are 3 orders of magnitude between the DOS associated with the current surface water chloride and when DOS = 1, indicating that under present-day conditions would likely take 100 s of years before the site tips into a sulfidic state.
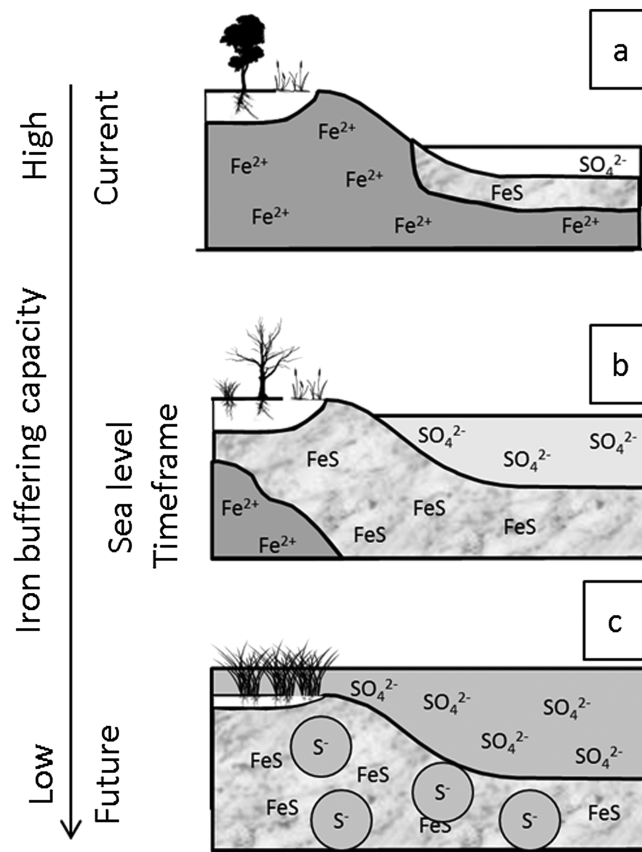
Figure 6. Conceptual model of iron buffering in a coastal freshwater wetland system undergoing salt water incursion. Representation of iron sulfur dynamics under (a) freshwater conditions and (b) salt water incursion, as well as (c) a transitional marsh.

4. Discussion

In coastal wetlands, iron acts as a buffering mechanism to sequester sulfide and prevent accumulation in sediments [*van der Welle et al.*, 2006, 2007]. Understanding the effectiveness and longevity of the iron buffer against sulfide is important for predicting the timing, magnitude, and direction of coastal wetland responses to salt water incursion and gradual sea level rise. Across our study site, extended exposure to marine salts led to only modest and temporary increases in the degree of sulfidization (DOS) due to the combined effects of a large soil iron pool that effectively sequesters sulfide and a modest degree of salt water incursion during our sampling period. Although we are certain that most low-lying coastal wetlands, such as the TOWeR wetland, will eventually become salt marshes as a consequence of sea level rise [*Craft et al.*, 2009], the fate of these ecosystems in the near term is far less predictable. Both droughts and storm surges can lead to significant landward movement of salt water into historically fresh coastal wetlands [*Ardón et al.*, 2010]. Salt water incursion introduces significant chemical stress to wetland plants, both directly through the addition of marine salts and indirectly through the stimulation of microbial sulfate reduction and the production of the potent phytotoxin sulfide [*Wang and Chapman*, 1999]. The relative importance of these two stressors during the early stages of salt water exposure depends to a large extent on the amount and reactivity of soil Fe pools.

The TOWeR wetland, especially the upper reach (Figure 1; Site 4), is predominantly a freshwater system that is able to support a diverse freshwater plant and microbial community. With the beginnings of salt water incursion (Figure 6a), the freshwater wetland will begin to produce sulfide as more sulfate becomes available to the microbial pool. However, the large soil iron pool (Table 1) will adsorb the sulfide and buffer against the build up of free sulfide by creating FeS complexes. In the seasonally brackish downstream reaches of the wetland (Figure 1; Site 1 salt), this iron pool has already absorbed sulfide produced during five previous years of salt water incursion [*Ardón et al.*, 2013] into iron sulfide complexes (Figure 6b); however, with additional salt water (Figure 6c), the sulfide will begin to saturate the iron pool and build up as free sulfide (H_2S) in the pore waters. This shift in chemical composition will be reflected in the plant and microbial community, which require specific adaptations to grow under high-sulfide conditions [*Wang and Chapman*, 1999]. Knowing iron and sulfate reduction rates and iron sulfide complex formation patterns will aid in determining the timeline and magnitude of the transition from a freshwater wetland to a salt water dominated community.

4.1. Salt Water Controls on Iron and Sulfate Reduction Rates and Products

Very few studies measure multiple parameters of coupled iron and sulfur cycling but rather tend to focus on one element. For example, we are not aware of a study that reports rates of iron and sulfur reduction (processes) as well as the pools of AVS, CVS, total iron, and DOS value. In comparison to other studies in coastal and estuarine wetlands, our mean iron reduction rates were low (1300–38,000 nmol Fe g soil^{-1} d^{-1} as

reported by *Lovley and Phillips* [1986] and *Bullock et al.* [2012]). Geometric mean sulfate reduction rates aligned with other values, both from salt and freshwater systems, were predominantly on the lower end of published values (5–8000 nmol cm^{-2} d^{-1} as reported by *Jorgensen and Bak* [1991] and *Howarth and Merkel* [1984]). Our DOS value is very low, congruent with low sulfate reduction rates and FeS pools combined with high soil iron. Increased information regarding the coupling of iron and sulfur cycling in coastal wetlands will be critical to understanding how these ecosystems will respond to climate change.

Across our site, patterns of both iron and sulfate reduction rates followed the rise and fall of surface water conductivity (Figure 2). As sulfate became available to sulfate-reducing bacteria due to an influx of saltier water, sulfate reduction also increased, suggesting that sulfate reducers were present in the wetland and were only sulfate limited. When the sulfate began to flush out of the wetland at the end of the season, sulfate reduction slowed to mirror this availability. Iron reduction also increased in response to high pore water chloride in sites that were continually submerged, indicating that salt water incursion and sea level rise are also likely to impact rates of iron reduction in coastal wetlands. Although iron reduction rates were lower in July, reduced iron concentrations were markedly higher than any other month, potentially indicating rapid reduction of much of the microbially available pool before our July measurements were taken (data not shown).

Both median acid volatile sulfide (AVS) and chromium reducible sulfur (CRS) decreased as the salt water incursion event intensified (Figure 4), presumably due to either sediment oxidation or consumption as electron donors. Sulfide complexes can act electron donors for nitrogen respiration (e.g., denitrification [*Brunet and Garcia-Gil*, 1996; *Haaijer et al.*, 2007; *Burgin et al.*, 2012]), and nitrogen retention is high at TOWeR [*Ardón et al.*, 2010], and loss of ammonium is related to salt water inputs at the outflow [*Ardón et al.*, 2013]. Although N cycling is certainly affected by salt water incursion, the degree of connection between nitrogen, sulfur, and iron (e.g., FeS) transformations remains unknown [*Burgin and Hamilton*, 2007]. Another nonmutually exclusive explanation of the low concentrations of reduced FeS complexes is oxidation via radial oxygen loss in plant roots [*Paul et al.*, 2006] or drying down with increased evapotranspiration in the summer. It is highly likely that the oxidation hypothesis is more plausible, as there is a disconnect between the location of salt and nitrogen at the site.

Moisture and water extractable chloride together were the strongest predictor of AVS concentrations (Table 2), indicating the importance of salt and reducing conditions in promoting AVS formation. CRS was more strongly related to water extractable chloride than moisture, especially at the surface (Table 2). It is possible that sulfate is not the limiting factor in FeS formation; rather, anoxic and warm conditions were needed to stimulate the microbes, and these factors correlate with salt water exposure. Variation in AVS and CRS concentrations increased with depth (data not shown). Deeper sediments are less likely to experience dry down, and thus, the higher concentrations of AVS and CRS at deeper depths are possible, due to the more stable reducing conditions. However, there is less salt water exposure at depth, which may counteract strong reducing conditions. This finding is congruent with our understanding that the site experiences surface-driven incursion and that there is more active sulfate reduction under highly reducing conditions and increased salt water exposure. AVS and CRS concentrations were very low throughout the study, generally <100 nmol g dry wt^{-1}, likely due to low salt water input and low background sulfate concentrations in surface waters.

4.2. How Much Salinization Is Required for a Sulfidic Wetland Transformation?

All attempts to estimate the chloride necessary to reach a DOS = 1 with present-day data are overly conservative since it also assumes no change in sea level and a stable water budget (i.e., no change in drought intensity); both factors that we know will change dramatically with impending climate change [*Nicholls and Cazenave*, 2010; *Seneviratne et al.*, 2002]. Since incursion is surface water driven, surface sediments may contain a higher DOS than deeper sediments at any given point during incursion. Also, the complex hydrology of the site, as is true for all wetlands, also needs to be incorporated into modeling efforts to extrapolate our findings to scaling efforts. At TOWeR, for example, areas closer to the main channel (Figure 1) will be more FeS saturated than the areas furthest from the channel. A more accurate prediction of the sulfidization tipping point for any soil should include water diffusion rates, as well as the rate iron will become microbially available for reduction due to chloride mediated solubility. Our conceptual analysis, however, provides a way to integrate and couple models of coastal wetland soil chemistry to sea level change hydrologic models. In reality, we predict a much more rapid progression from the freshwater to a saline system.

AVS and CRS comprise two of the major sinks of sulfur in wetland sediments [*King*, 1988]. A third potential pool, free sulfide (H_2S) can build up under certain conditions, but free sulfide was not observed in our concurrent monitoring of shallow (15 cm deep) groundwater wells (data not shown). We did occasionally observe pore water sulfide in very near-surface areas (e.g., <3 cm depth) in areas under persistent salt water incursion; this, however, was relatively rare and isolated to areas near the salt water source on the site [*Hopfensperger et al.*, 2014].

In contrast to other studies in sites exposed continuously to high-sulfate loading, the DOS at TOWeR is very low (reaching a maximum of 0.0014). In the Baltic Sea, CRS reached 30 µmol g dry wt^{-1} and had a DOS of up to 0.60. By comparison, the DOS of Baltic sediments are high; however, it is a saline system with much higher sulfate concentrations, which leads to a larger proportion of sulfide in an iron-limited environment [*Boesen and Postma*, 1988]. AVS ranged from 0 to 60 µmol g dry wt^{-1} and CRS ranged from 20 to 100 µmol g dry wt^{-1} in Texas estuaries, with total iron ranging from 40 to 600 µmol g dry wt^{-1} which resulted in DOS of 0–1.65 [*Morse et al.*, 2007]. In a freshwater system impacted by mining, DOS values ranged up to 0.7, indicating low-iron and high-sulfide concentrations [*Huerta-Diaz et al.*, 1998].

Little work has been done worldwide to characterize the extent of sulfidization along the world's freshwater coasts. Great efforts have determined the rate of physical sea level rise; however the potential chemical effects remain much less understood. In certain areas, such as the southeastern United States, wetland sediments are high in iron [*Johnston and Crossley*, 2002]. This iron has the potential to buffer the wetland against the sulfidic effects of sea level rise. Much of coastal North Carolina, including the TOWeR site, is under 1 m in elevation, and with projected sea level rise, North Carolina is expected to lose over 4500 km^2 of land area in the next 100 years [*Poulter and Halpin*, 2008]. Taking this into consideration, a physical incursion of the TOWeR wetland will perhaps occur before complete sulfidization of the sediment. Thirteen percent of the land area in the United States is composed of this iron-rich, Ultisol soil, which can become partially sulfidic simply from periodic drought [*Wilding et al.*, 1983]. In certain areas of the world (e.g., Australia), many soils are already sulfidic [*Fitzpatrick et al.*, 2009]; these areas are seeing the chemical consequences of sea level rise on much shorter time scales. Further research on connecting the hydrologic drivers of climate change with coastal wetland biogeochemical models is needed to predict how coastal areas will respond to impending sea level rise.

References

Allen, H., G. Fu, and B. Deng (1993), Analysis of acid volatile sulfide (AVS) and simultaneously extracted metals (SEM) for the estimation of potential toxicity in aquatic sediments, *Environ. Toxicol. Chem.*, *12*, 1441–1453, doi:10.1002/etc.5620120812.

Ardón, M., J. L. Morse, M. W. Doyle, and E. S. Bernhardt (2010), The water quality consequences of restoring wetland hydrology to a large agricultural watershed in the southeastern coastal plain, *Ecosystems*, *13*(7), 1060–1078, doi:10.1007/s10021-010-9374-x.

Ardón, M., J. L. Morse, B. P. Colman, and E. S. Bernhardt (2013), Drought-induced saltwater incursion leads to increased wetland nitrogen export, *Global Change Biol.*, *19*(10), 2976–2985, doi:10.1111/gcb.12287.

Boesen, C., and D. Postma (1988), Pyrite formation in anoxic environments of the Baltic, *Am. J. Sci.*, *288*, 575–603, doi:10.2475/ajs.288.6.575.

Brock, M. A., D. L. Nielsen, and K. Crossle (2005), Changes in biotic communities developing from freshwater wetland sediments under experimental salinity and water regimes, *Freshwater Biol.*, *50*(8), 1376–1390, doi:10.1111/j.1365-2427.2005.01408.x.

Brunet, R. C., and L. J. Garcia-Gil (1996), Sulfide-induced dissimilatory nitrate reduction to ammonia in anaerobic freshwater sediments, *FEMS Microbiol. Ecol.*, *21*(2), 131–138, doi:10.1111/j.1574-6941.1996.tb00340.x.

Bullock, A. L., A. E. Sutton-Grier, and J. P. Megonigal (2012), Anaerobic metabolism in tidal freshwater wetlands: III. Temperature regulation of iron cycling, *Estuaries Coasts*, doi:10.1007/s12237-012-9536-5.

Burgin, A., and S. Hamilton (2007), Have we overemphasized the role of denitrification in aquatic ecosystems? A review of nitrate removal pathways, *Front. Ecol. Environ.*, *5*(2), 89–96, doi:10.1890/1540-9295(2007)5[89:HWOTRO]2.0.CO;2.

Burgin, A., S. Hamilton, S. Jones, and J. Lennon (2012), Denitrification by sulfur-oxidizing bacteria in a eutrophic lake, *Aquat. Microb. Ecol.*, *66*(3), 283–293, doi:10.3354/ame01574.

Burton, E. D., R. T. Bush, and L. A. Sullivan (2006), Fractionation and extractability of sulfur, iron and trace elements in sulfidic sediments, *Chemosphere*, *64*(8), 1421–1428, doi:10.1016/j.chemosphere.2005.12.003.

Connell, W., and W. Patrick Jr. (1968), Sulfate reduction in soil: Effects of redox potential and pH, *Science*, *159*(3810), 86–87.

Craft, C., J. Clough, J. Ehman, S. Joye, R. Park, S. Pennings, H. Guo, and M. Machmuller (2009), Forecasting the effects of accelerated sea-level rise on tidal marsh ecosystem services, *Front. Ecol. Environ.*, *7*(2), 73–78, doi:10.1890/070219.

Donahoe, R., and C. Liu (1998), Pore water geochemistry near the sediment-water interface of a zoned, freshwater wetland in the southeastern United States, *Environ. Geol.*, *33*, 143–153, doi:10.1007/s002540050234.

Fitzpatrick, R. W., P. Shand, and R. H. Merry (2009), Acid sulfate soils, in *Natural History of the Riverland and Murraylands*, pp. 65–111, Royal Society of South Australia, Adelaide, South Australia.

Fossing, H., and B. Jørgensen (1989), Measurement of bacterial sulfate reduction in sediments: Evaluation of a single-step chromium reduction method, *Biogeochemistry*, *8*(3), 205–222, doi:10.1007/BF00002889.

Golterman, H. L. (1991), Influence of FeS on denitrification in shallow waters, *Verh. Int. Ver. Limnol.*, *24*, 3025–3028.

Haaijer, S. C. M., L. P. M. Lamers, A. J. P. Smolders, M. S. M. Jetten, H. J. M. Camp, and O. Den (2007), Iron sulfide and pyrite as potential electron donors for microbial nitrate reduction in freshwater wetlands, *Geomicrobiol. J.*, *24*(5), 391–401, doi:10.1080/01490450701436489.

Hopfensperger, K. N., A. J. Burgin, V. A. Schoepfer, and A. M. Helton (2014), Impacts of saltwater incursion on plant communities, anaerobic microbial metabolism, and resulting relationships in a restored freshwater wetland, *Ecosystems*, doi:10.1007/s10021-014-9760-x.

Howarth, R. W., and S. Merkel (1984), Pyrite formation and the measurement of sulfate reduction in salt marsh sediments, *Limnol. Oceanogr.*, *29*, 598–608.

Huerta-Diaz, M., A. Tessier, and R. Carignan (1998), Geochemistry of trace metals associated with reduced sulfur in freshwater sediments, *Appl. Geochem.*, *13*(2), 213–233, doi:10.1016/S0883-2927(97)00060-7.

Johnston, J., and D. Crossley (2002), Forest ecosystem recovery in the southeast US: Soil ecology as an essential component of ecosystem management, *For. Ecol. Manage.*, *155*, 187–203, doi:10.1016/S0378-1127(01)00558-8.

Jorgensen, B. B., and F. Bak (1991), Pathways and microbiology of thiosulfate transformation and sulfate reduction in a marine sediment (Kattegat, Denmark), *Appl. Environ. Microbiol.*, *57*, 847–856.

King, D., and D. B. Nedwell (1985), The influence of nitrate concentration upon the end-products of nitrate dissimilation by bacteria in anaerobic salt marsh sediment, *FEMS Microbiol. Ecol.*, *31*, 23–28.

King, G. (1988), Patterns of sulfate reduction and the sulfur cycle in a South Carolina salt marsh, *Limnol. Oceanogr.*, *33*(3), 376–390, doi:10.4319/lo.1988.33.3.0376.

Lamers, L. P. M., L. L. Govers, I. C. J. M. Janssen, J. J. M. Geurts, M. E. W. Van der Welle, M. M. Van Katwijk, T. Van der Heide, J. G. M. Roelofs, and A. J. P. Smolders (2013), Sulfide as a soil phytotoxin—A review, *Front. Plant Sci.*, *4*(July), 1–14, doi:10.3389/fpls.2013.00268.

Liu, X., and F. J. Millero (1999), The solubility of iron hydroxide in sodium chloride solutions, *Geochim. Cosmochim. Acta*, *63*(19), 3487–3497, doi:10.1016/S0016-7037(99)00270-7.

Liu, X., and F. J. Millero (2002), The solubility of iron in seawater, *Mar. Chem.*, *77*, 43–54.

Lord, C., and T. Church (1983), The geochemistry of salt marshes: Sedimentary ion diffusion, sulfate reduction, and pyritization, *Geochim. Cosmochim. Acta*, *47*, 1381–1391, doi:10.1016/0016-7037(83)90296-X.

Lovley, D. R. (1991), Dissimilatory Fe(Iii) and Mn(Iv) reduction, *Microbiol. Rev.*, *55*(2), 259–287, doi:10.1016/S0065-2911(04)49005-5.

Lovley, D. R., and E. J. P. Phillips (1986), Organic matter mineralization with reduction of ferric iron in anaerobic sediments, *Appl. Environ. Microbiol.*, *51*(4), 683–689.

Megonigal, J., and S. Neubauer (2009), Biogeochemistry of tidal freshwater wetlands, in *Coastal Wetlands: An Integrated Ecosystems Approach*, edited by G. Perillo et al., p. 535, Elsevier, Amsterdam.

Morse, J. L., M. Ardón, and E. Bernhardt (2012), Greenhouse gas fluxes in southeastern US coastal plain wetlands under contrasting land uses, *Ecol. Appl.*, *22*(1), 264–280, doi:10.1890/11-0527.1.

Morse, J. W., H. Thomson, and D. W. Finneran (2007), Factors controlling sulfide geochemistry in sub-tropical estuarine and bay sediments, *Aquat. Geochem.*, *13*(2), 143–156, doi:10.1007/s10498-007-9012-1.

Neubauer, S. C., K. Givler, S. Valentine, and J. P. Megonigal (2005), Seasonal patterns and plant-mediated controls of subsurface wetland biogeochemistry, *Ecology*, *86*(12), 3334–3344, doi:10.1890/04-1951.

Nicholls, R. J., and A. Cazenave (2010), Sea-level rise and its impact on coastal zones, *Science*, *328*(5985), 1517–1520, doi:10.1126/science.1185782.

Odum, W. E. (1988), Comparative ecology of tidal freshwater and salt marshes, *Annu. Rev. Ecol. Syst.*, *19*, 147–176.

Paul, S., K. Kusel, and C. Alewell (2006), Reduction processes in forest wetlands: Tracking down heterogeneity of source/sink functions with a combination of methods, *Soil Biol. Biochem.*, *38*(5), 1028–1039, doi:10.1016/j.soilbio.2005.09.001.

Pezeshki, S. R. (2001), Wetland plant responses to soil flooding, *Environ. Exp. Bot.*, *46*(3), 299–312, doi:10.1016/S0098-8472(01)00107-1.

Poulter, B., and P. N. Halpin (2008), Raster modelling of coastal flooding from sea-level rise, *Int. J. Geogr. Inf. Sci.*, *22*(2), 167–182, doi:10.1080/13658810701371858.

Rabenhorst, M. C., J. P. Megonigal, and J. Keller (2010), Synthetic iron oxides for documenting sulfide in marsh pore water, *Soil Sci. Soc. Am. J.*, *74*(4), 1383–1388, doi:10.2136/sssaj2009.0435.

R Core Team (2012), *R: A Language and Environment for Statistical Computing*, R Foundation for Statistical Computing, Vienna, Austria. [Available at http://www.R-projct.org/.]

Seneviratne, S., J. Pal, E. Eltahir, and C. Schar (2002), Summer dryness in a warmer climate: A process study with a regional climate model, *Clim. Dyn.*, *20*(1), 69–85, doi:10.1007/s00382-002-0258-4.

Stumm, W., and J. J. Morgan (1996), *Aquatic Chemistry, Chemical Equilibria and Rates in Natural Waters*, 3rd ed., 1022 pp., John Wiley, New York.

Van der Welle, M. E. W., M. Cuppens, L. P. M. Lamers, and J. G. M. Roelofs (2006), Detoxifying toxicants: Interactions between sulfide and iron toxicity in freshwater wetlands, *Environ. Toxicol. Chem.*, *25*(6), 1592–1597. [Available at http://www.ncbi.nlm.nih.gov/pubmed/16764478.]

Van der Welle, M. E. W., A. J. P. Smolders, H. J. M. Op Den Camp, J. G. M. Roelofs, and L. P. M. Lamers (2007), Biogeochemical interactions between iron and sulphate in freshwater wetlands and their implications for interspecific competition between aquatic macrophytes, *Freshwater Biol.*, *52*(3), 434–447, doi:10.1111/j.1365-2427.2006.01683.x.

Wang, F. Y., and P. M. Chapman (1999), Biological implications of sulfide in sediment—A review focusing on sediment toxicity, *Environ. Toxicol. Chem.*, *18*(11), 2526–2532, doi:10.1002/etc.5620181120.

Werner, A. D., M. Bakker, V. E. A. Post, A. Vandenbohede, C. Lu, B. Ataie-Ashtiani, C. T. Simmons, and D. A. Barry (2013), Seawater intrusion processes, investigation and management: Recent advances and future challenges, *Adv. Water Resour.*, *51*, 3–26, doi:10.1016/j.advwatres.2012.03.004.

Weston, N. B., R. E. Dixon, and S. B. Joye (2006), Ramifications of increased salinity in tidal freshwater sediments: Geochemistry and microbial pathways of organic matter mineralization, *J. Geophys. Res.*, *111*, G01009, doi:10.1029/2005JG000071.

Wijsman, J., and J. Middelburg (2001), Sulfur and iron speciation in surface sediments along the northwestern margin of the Black Sea, *Mar. Chem.*, *74*, 261–278.

Wilding, L. P., N. E. Smeck, and G. F. Hall (1983), *Pedogenesis and Soil Taxonomy I. Concepts and Interactions*, Elsevier Sci. Publ., New York.